APPLIED PHYSICS LETTERS 107, 072101 (2015)

Extracting the effective bandgap of heterojunctions using Esaki diode I-V measurements

Quentin Smets,[1,2,a)] Anne S. Verhulst,[1] Salim El Kazzi,[1] Devin Verreck,[1,2] Olivier Richard,[1] Hugo Bender,[1] Nadine Collaert,[1] Anda Mocuta,[1] Aaron Thean,[1] and Marc M. Heyns[1,2]
[1]Imec, Kapeldreef 75, 3001 Heverlee, Belgium
[2]KULeuven, 3000 Leuven, Belgium

(Received 16 June 2015; accepted 7 August 2015; published online 17 August 2015)

The effective bandgap is a crucial design parameter of heterojunction tunneling field-effect transistors. In this letter, we demonstrate a method to measure the effective bandgap directly from the band-to-band tunneling current of a heterojunction Esaki diode, of which we only require knowledge of the electrostatic potential profile. The method is based on a characteristic exponentially increasing current with forward bias, caused by sharp energy filtering at cryogenic temperature. We apply this method experimentally to a n+$In_{0.53}Ga_{0.47}As$/p$GaAs_{0.5}Sb_{0.5}$ Esaki diode and define requirements to apply it to other heterojunctions. © *2015 AIP Publishing LLC*.
[http://dx.doi.org/10.1063/1.4928761]

The effective bandgap ($E_{g,eff}$, inset of Fig. 1) of heterojunctions is a crucial design parameter for Resonant Interband Tunneling Diodes (RITD) for high speed analog applications[1] and Tunneling Field-Effect Transistors (TFET) for ultra low power logic.[2] $E_{g,eff}$ is usually determined from the electron affinities and bandgaps of the bulk materials,[3] or using optical measurements.[4,5] However, there is significant uncertainty on $E_{g,eff}$, especially for the heterostructure $In_{0.53}Ga_{0.47}As$/$GaAs_{0.5}Sb_{0.5}$ (InGaAs/GaAsSb, Fig. 1), which makes the prediction of TFET performance difficult.[6] The lattice-matched $In_xGa_{1-x}As$/$GaAs_{1-y}Sb_y$ heterojunction system is promising for TFET[3,7–13] due to its tunable $E_{g,eff}$ (Fig. 1). In this letter, we present and experimentally demonstrate a method to measure $E_{g,eff}$ directly from the Band-To-Band Tunneling current density (J_{BTBT}) of a InGaAs/GaAsSb Esaki diode.

The method requires a p+/n or p/n+ Esaki diode (Figs. 2(a) and 2(c)) with a staggered (type II) or straddled (type I) band alignment, of which the highly doped region is highly degenerate and the lowly doped region is lowly degenerate or non-degenerate. Semiclassical[14] (Figs. 2(b) and 2(d)) and Quantum Mechanical[15] (QM) simulations at cryogenic temperature show a nearly exponentially increasing BTBT current with more negative reverse bias $0 > V_{np} > V_c$, which is unusual for p+/n+ Esaki diodes. V_c is the voltage where BTBT no longer increases exponentially and can easily be recognized visually. It will be theoretically shown that $E_{g,eff}$ can be extracted from V_c without requiring knowledge of the bandgaps or tunneling rates.

In order to intuitively understand the origin of the exponentially increasing current, we theoretically derive the approximate I–V relation for p/n+ diodes (Fig. 2(a)). A similar derivation can be made for p+/n diodes (Fig. 2(c)). The exponential current originates from a sharp energy filtering mechanism. Tunneling occurs dominantly at $E = E_{fp}$, along a path which starts at the hetero-interface and ends in the lowly p-type doped material (Fig. 2(a)). Tunneling at the highest energy levels ($E > E_{fp}$) is suppressed because these tunnel paths are longer (Fig. 3(a)). At cryogenic temperature, tunneling at $E < E_{fp}$ is also suppressed due to a reduced amount of empty states 1-f_{FDp} (E), with f_{FDp} (E) the Fermi-Dirac occupation in the p-type region. This causes a peak in tunneling near E_{fp}. The BTBT current can therefore be described by considering tunneling only at this energy and using the Wentzel-Kramer-Brillouin (WKB) approximation

$$J_{BTBT} \propto \exp\left(-2\int_0^L \kappa\, dx\right), \quad (1)$$

where κ is the magnitude of the imaginary wavevector k along the tunnel path in the forbidden gap[16] and L is the length of the tunnel path. Due to the quadratic band bending in GaAsSb (Fig. 4(a)), the shape of $\kappa(x)$ in GaAsSb remains unchanged with more negative V_{np}, and only the limits of the integration change. For $0 > V_{np} > V_c$, the value of $\kappa(x=0)$ is nearly constant because the tunnel path starts close to midgap. We can locally approximate that L decreases linearly with $-V_{np}$ down to V_c (Fig. 4(c)). This causes J_{BTBT} to increase nearly exponentially (Fig. 4(b)). When $V_{np} < V_c$, the tunnel path extends into InGaAs and the current no longer increases exponentially, which allows the visual extraction of V_c from the I–V curve. More rigorous simulations with a fully QM 15-band k·p solver[15] (not shown) confirm the same trends in the I–V curve. Contrary to the WKB approximation, the QM simulations do not neglect wavefunction reflections due to the discontinuity in $\kappa(x)$ at the heterointerface.[17,18]

We can easily extract $E_{g,eff}$ from V_c, because at this bias condition, E_c of InGaAs at the hetero-interface is equal to E_{fp} (Fig. 4(a)). Therefore, we obtain the relation

$$E_{g,eff} = q(\Delta\Psi_n + \Delta\Psi_p - V_c) - \xi_n - \xi_p, \quad (2)$$

where q is the elementary charge, $\Delta\Psi_n$, $\Delta\Psi_p$ are the band bending of the n and p regions at $V_{np} = V_c$ (Fig. 4(a)), and the degeneracies are $\xi_n = E_{fn}-E_{c,n,bulk}$ and $\xi_p = E_{v,p,bulk}-E_{fp}$ or zero if non-degenerate. In order to be valid for staggered and straddled heterojunctions, we define the effective

a)Electronic mail: quentin.smets@imec.be

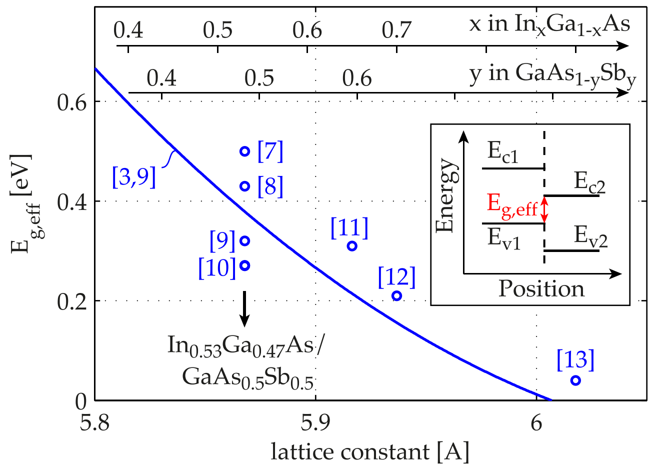

FIG. 1. Many lattice matched $In_xGa_{1-x}As/GaAs_{1-y}Sb_y$ heterojunction TFETs have been demonstrated in literature, but there is significant uncertainty on the reported $E_{g,eff}$. The full line is calculated from electron affinities and bandgaps of the bulk materials.[3,9]

bandgap at the hetero-interface as $E_{g,eff} = E_{c,n} - E_{v,p}$ with $E_{c,n}$ the n-type region conduction band edge and $E_{v,p}$ the p-type region valence band edge, both taken at the hetero-interface (Figs. 2(a) and 2(c)).

Four requirements are identified to obtain nearly exponentially increasing current in p/n+ Esaki diodes. First, the temperature must be sufficiently low (Fig. 3(b)). Simulations show the required temperature decreases with higher p-type dopant concentration, lower $E_{g,eff}$, and higher degeneracy ξ_p. Experimentally this required temperature can be found easily

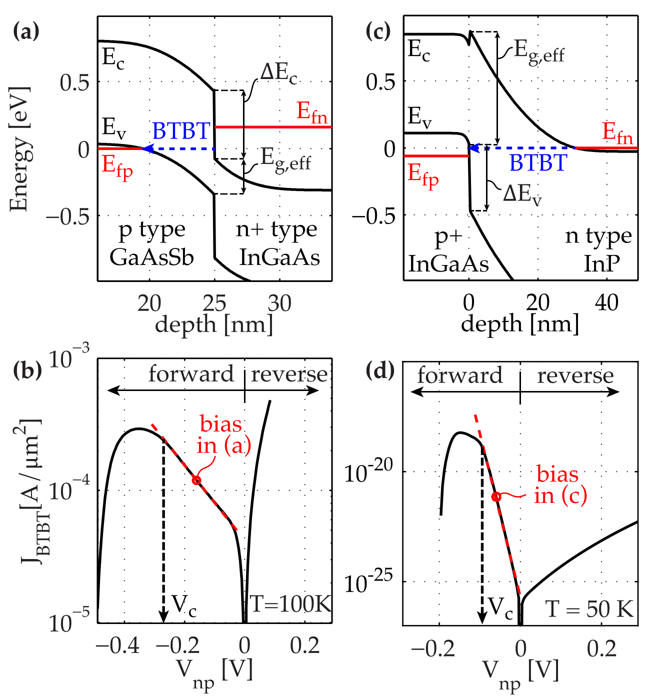

FIG. 2. (a) The band diagram of a forward biased p/n+ Esaki diode with staggered alignment shows tunneling from the heterointerface to the lowly doped region. E_c, E_v are conduction and valence band edges and E_{fn}, E_{fp} are the quasi Fermi energy levels. (b) The corresponding simulation[14] shows J_{BTBT} increases exponentially with forward bias at sufficiently low temperature. (c) and (d) Similar behavior for a p+/n heterojunction with straddled alignment.

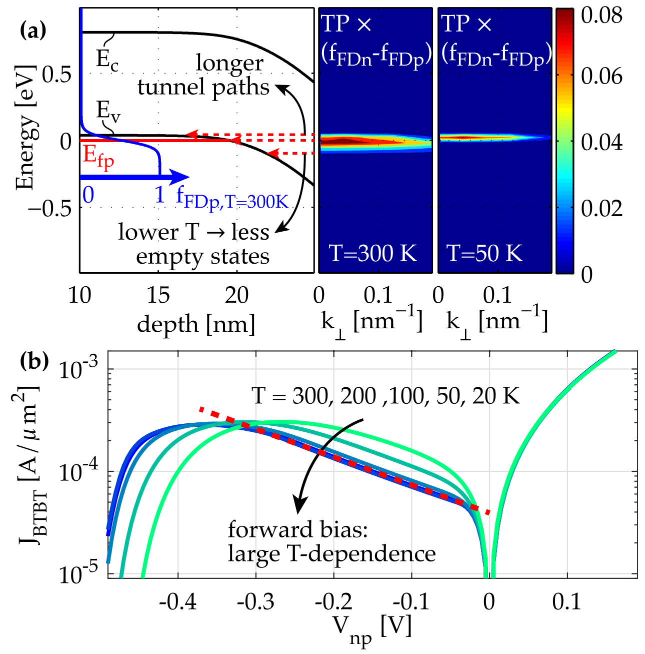

FIG. 3. (a) The dashed arrows in the GaAsSb band diagram show suppressed tunneling at $E > E_{fp}$ and $E < E_{fp}$. The Transmission Probability (TP) weighted with Fermi-Dirac shows a peak in tunneling near E_{fp} at $T = 50$ K. The TP is calculated with a 15-band k·p solver[15] and $k_\perp$ is the wavevector perpendicular to the tunneling direction. (b) Simulations[14] show that at small forward bias, J_{BTBT} is temperature dependent for $T > 100$ K and exponential for $T < 100$ K.

by performing I–V measurements and lowering the temperature until the I–V no longer changes. Second, intermixing of both semiconductors near the heterointerface must be sufficiently low. Simulations show that the current is no longer exponential if the intermixing region is larger than 1 nm. Third, the degeneracy ξ_n must be larger than the band bending of the n+ region ($\Delta\Psi_n$ in Fig. 4(a)) at $V_{np} = 0$. This is easily achieved in n+InGaAs due to its low conduction band density of states, but not in n+silicon. Finally, the conduction band offset at the hetero-interface (ΔE_c in Fig. 2(a)) must be positive and sufficiently large ($q\Delta E_c > \xi_n - q\Delta\Psi_n$) such that the tunnel path starts at the heterointerface at $V_{np} = 0$. This is the case for n+InGaAs/pGaAsSb but not for n+InGaAs/pInP. Furthermore, simulations show that the method remains valid in the limit of a near-broken bandgap heterojunction with $E_{g,eff} = 0$ eV.

We experimentally verify our prediction of exponential BTBT current in a forward biased diode.[6] An InGaAs/GaAsSb heterojunction is grown on a lattice matched InP substrate with Molecular Beam Epitaxy (MBE) as described in Ref. 20. The active dopant concentrations $n = 3.3 \times 19^{19} cm^{-3}$ and $p = 1.1 \times 19^{19} cm^{-3}$ are obtained with Hall measurements and satisfy the previously mentioned requirements for exponential BTBT current. Transmission Electron Microscopy (HR-HAADF-STEM, Fig. 5) analysis confirms a sharp hetero-interface with less than 1 nm of intermixing. Diodes with junction areas $A_j = 0.01$–$2\,\mu m^2$ are fabricated according to the process flow in Ref. 21. We measure the diode I-V characteristics with an *Agilent 4156C* parameter analyzer. Perimeter effects are negligible, since I_{BTBT} scales with A_j in reverse (inset of Fig. 6) and forward bias, but only after correction for series resistance R_s according to the

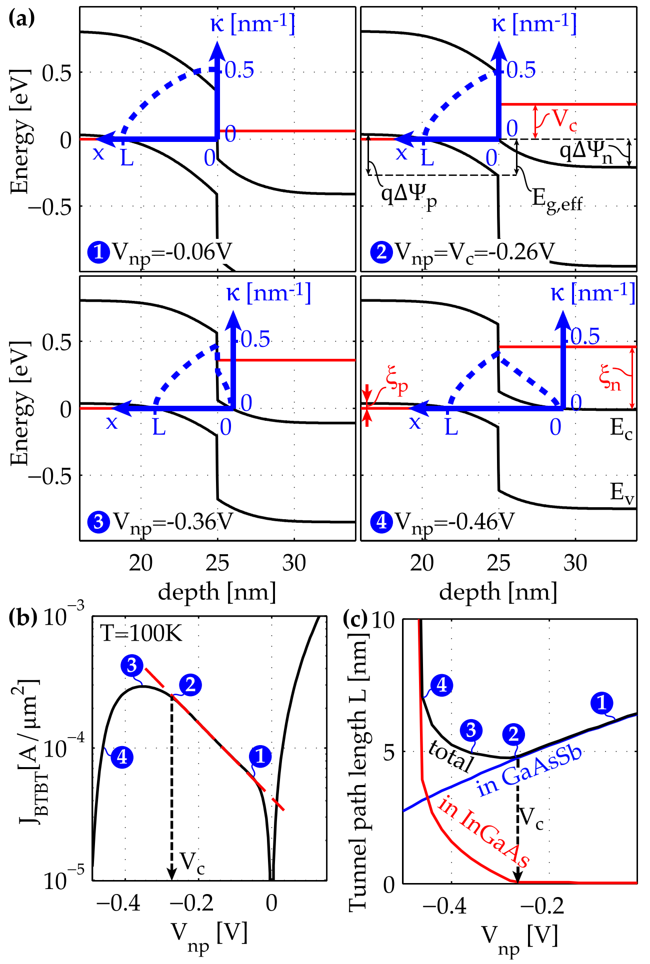

FIG. 4. (a) and (c) The tunnel path at $E = E_{fp}$ is located entirely in GaAsSb for $0 > V_{np} > V_c$, and extends to InGaAs for $V_{np} < V_c$. κ is calculated using the Kane 2-band dispersion relation.[19] (b) The current no longer increases exponentially when $V_{np} < V_c$.

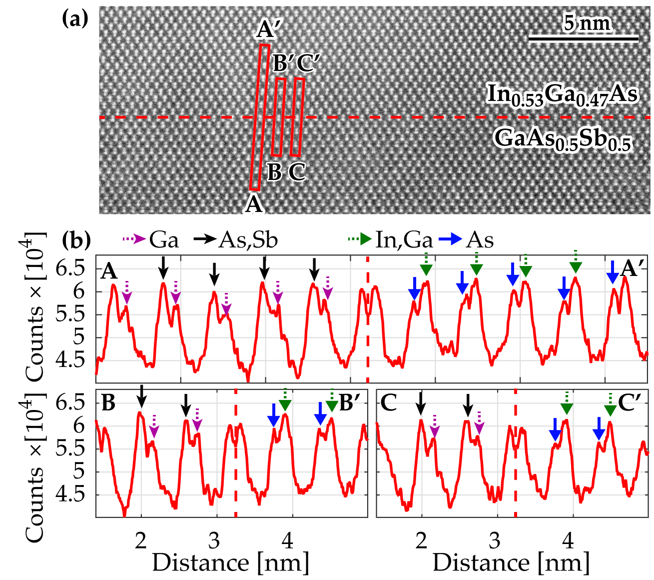

FIG. 5. (a) HR-HAADF-STEM analysis and (b) the intensity traces along A-A′, B-B′, and C-C′ show a locally smooth and sharply defined heterointerface with an intermixing region smaller than 1 nm and no visible defects.

procedure described in Ref. 20. The measured V_c can be severely impacted by a high R_s if the I–V curves are not corrected.[6] While the peak voltage of diodes with $A_j = 0.04\ \mu m^2$ shifts by only 0.02 V, diodes with $A_j = 2\ \mu m^2$ carry more current and the peak voltage is shifted by 0.1 V when correcting for $R_s = 350\ \Omega$. When the temperature is lowered, we observe a decrease of BTBT in forward bias, and the I–V becomes more exponential (Fig. 6) as predicted by simulations (Fig. 3(b)). The exponential current also confirms that the intermixing region at the heterojunction is smaller than 1 nm. At T = 78 K, we extract $V_c = -0.27$ V from 4 diodes with different areas.

In order to extract $E_{g,eff}$ from V_c using Eq. (2), we calculate the degeneracies $\xi_{n,p}$ and band bending $\Delta\Psi_{n,p}$ at V_c using the measured active dopant concentrations and Sentaurus Device.[14] We use Fermi-Dirac statistics and the effective mass approximation for the light hole, heavy hole, and conduction bands with a nonparabolicity correction in the Γ, L, and X valleys.[3,9,22] We assume dopant-dependent bandgap narrowing (dopant-BGN) does not increase the degeneracy, and we obtain $\xi_n = 0.47$ eV and $\xi_p = 0.04$ eV at T = 78 K. We obtain a match between simulated and measured $V_c = -0.27$ V at T = 78 K with $E_{g,eff} = 0.27$ eV. We then extrapolate this result to T = 300 K using literature data on temperature dependent bandgap narrowing[23,24] and obtain $E_{g,eff} = 0.21$ eV. Currently, we cannot quantitatively compare the full measured and simulated I–V, since this requires a profound understanding of dopant-BGN on BTBT rates.

We assess the sensitivity of $E_{g,eff}$ to the different input parameters in Eq. (2) using semiclassical simulations. If an error $\Delta V_c = \pm 20$ mV is made during the experimental extraction in Fig. 6, this results in an error $\Delta E_{g,eff} = \pm 45$ meV. If an error is made on ξ_n, ξ_p due to a possibly inaccurate density of states model, $\Delta\xi_p = \pm 20$ meV results in an error $\Delta E_{g,eff} = \mp 20$ meV, and $\Delta\xi_n = \pm 20$ meV results in $\Delta E_{g,eff} = \pm 11$ meV.

Even when considering these possible error bars, our obtained $E_{g,eff}$ is lower than other literature values for the undoped $In_{0.53}Ga_{0.47}As/GaAs_{0.5}Sb_{0.5}$ heterojunction[7–10] ($E_{g,eff} = 0.27$–0.5 eV, see Fig. 1). We identify three possible explanations for this discrepancy: First, dopant-BGN could

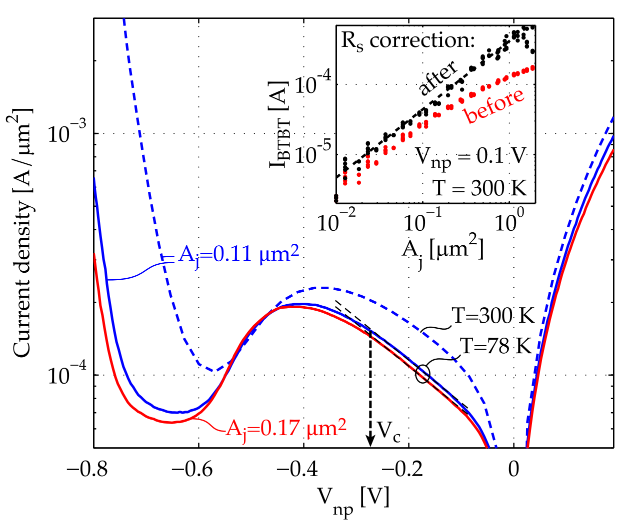

FIG. 6. The measured I-V curves become more exponential at T = 78 K. We extract $V_c = -0.27$ V from 2 diodes with different areas. The inset shows I_{BTBT} scales with the junction area, but only after correcting for series resistance.

increase ξ_n and ξ_p and therefore also $\Delta\Psi_{n,p}$. This would result in a underestimated $E_{g,eff}$ for the same measured $V_c = -0.27$ V. Our obtained value $E_{g,eff} = 0.21$ eV is therefore a lower limit.

Second, heavy doping could shift ΔE_c and ΔE_v and decrease $E_{g,eff}$.[25] Further extrapolation to an undoped heterojunction using literature values of Jain Roulston dopant-BGN[25,26] results in $E_{g,eff} = 0.39$ eV, which brings our measured value in the range found in literature.

The third possibility is a fixed interface charge affecting the band bending, as reported in Ref. 5 for a $In_{0.7}Ga_{0.3}As$/$GaAs_{0.35}Sb_{0.65}$ heterojunction. It was reported that a fixed positive charge of $6 \times 10^{12}\,cm^{-2}$ changed the band alignment from staggered to broken. However, HR-HAADF-STEM analysis shows no visible defects in our diodes (Fig. 5), thus we do not expect fixed charge to affect the measured $E_{g,eff}$.

In conclusion, simulations and experiments of heterojunction Esaki diodes at cryogenic temperature demonstrate a characteristic exponentially increasing BTBT current. It allows us to determine a lower limit $E_{g,eff} > 0.21$ eV for the $n+In_{0.53}Ga_{0.47}As/pGaAs_{0.5}Sb_{0.5}$ heterojunction using a method that requires knowledge of the dopant concentrations and degeneracies $\xi_{n,p}$ but not the bandgaps and tunnel rates. The exponential current also allows us to determine that the intermixing region at the junction is <1 nm, which is verified by HR-HAADF-STEM analysis. Other applications include the analysis of fixed charge at the heterojunction and further understanding of dopant-BGN and its impact on TFET.

Q. Smets and D. Verreck gratefully acknowledge the support of IWT-Vlaanderen. This work was supported by imec's industrial affiliation program.

[1]B. R. Bennett, R. Magno, J. B. Boos, W. Kruppa, and M. G. Ancona, "Antimonide-based compound semiconductors for electronic devices: A review," Solid-State Electron. **49**, 1875 (2005).
[2]H. Lu and A. Seabaugh, IEEE J. Electron Devices Soc. **2**, 44 (2014).
[3]I. Vurgaftman, J. R. Meyer, and L. R. Ram-Mohan, J. Appl. Phys. **89**, 5815 (2001).
[4]J. Klem, S. Kurtz, and A. Datye, "Growth and properties of GaAsSb/InGaAs superlattices on InP," J. Cryst. Growth **111**, 628 (1991).
[5]Y. Zhu, N. Jain, S. Vijayaraghavan, D. K. Mohata, S. Datta, D. Lubyshev, J. M. Fastenau, A. K. Liu, N. Monsegue, and M. K. Hudait, J. Appl. Phys. **112**, 094312 (2012).
[6]Q. Smets, A. S. Verhulst, S. E. Kazzi, A. Mocuta, and M. M. Heyns, in Device Research Conference, 2015.
[7]D. Mohata, S. Mookerjea, A. Agrawal, Y. Li, T. Mayer, V. Narayanan, A. Liu, D. Loubychev, J. Fastenau, and S. Datta, Appl. Phys. Express **4**, 024105 (2011).
[8]B. Romanczyk, P. Thomas, D. Pawlik, S. L. Rommel, W.-Y. Loh, M. H. Wong, K. Majumdar, W.-E. Wang, and P. D. Kirsch, Appl. Phys. Lett. **102**, 213504 (2013).
[9]V. Siklitsky, see http://www.ioffe.ru/SVA/NSM/Semicond/.
[10]T. Yu, J. T. Teherani, D. A. Antoniadis, and J. L. Hoyt, IEEE Electron Device Lett. **34**, 1503 (2013).
[11]B. Rajamohanan, R. Pandey, V. Chobpattana, C. Vaz, D. Gundlach, K. P. Cheung, J. Suehle, S. Stemmer, and S. Datta, IEEE Electron Device Lett. **36**(1), 20–22 (2015).
[12]D. Mohata, B. Rajamohanan, T. Mayer, M. Hudait, J. Fastenau, D. Lubyshev, A. W. K. Liu, and S. Datta, IEEE Electron Device Lett. **33**, 1568 (2012).
[13]R. Bijesh, H. Liu, H. Madan, D. Mohata, W. Li, N. V. Nguyen, D. Gundlach, C. A. Richter, J. Maier, K. Wang, T. Clarke, J. M. Fastenau, D. Loubychev, W. K. Liu, V. Narayanan, and S. Datta, IEEE IEDM **7**, 28.2.1–28.2.4 (2013).
[14]Synopsys, Sentaurus Device J-2014.09.
[15]D. Verreck, M. Van de Put, B. Sorée, A. S. Verhulst, W. Magnus, W. G. Vandenberghe, N. Collaert, A. Thean, and G. Groeseneken, J. Appl. Phys. **115**, 053706 (2014).
[16]S. M. Sze, *Physics of Semiconductor Devices*, 2nd ed. (Wiley, New York, 1981), p. 521.
[17]M. Van de Put, in *Eurocon* (2013), pp. 2134–2139.
[18]A. Ajoy, in *15th International Workshop on Computational Electronics, IWCE 2012* (2012), pp. 2–5.
[19]E. O. Kane, J. Appl. Phys. **32**, 83 (1961).
[20]S. El Kazzi, Q. Smets, M. Ezzedini, R. Rooyackers, A. Verhulst, B. Douhard, H. Bender, N. Collaert, C. Merckling, M. Heyns, and A. Thean, J. Cryst. Growth **424**, 62 (2015).
[21]Q. Smets, D. Verreck, A. S. Verhulst, R. Rooyackers, C. Merckling, M. Van De Put, E. Simoen, W. Vandervorst, N. Collaert, V. Y. Thean, B. Sorée, G. Groeseneken, and M. M. Heyns, J. Appl. Phys. **115**, 184503 (2014).
[22]V. A. Altschul, A. Fraenkel, and E. Finkman, J. Appl. Phys. **71**, 4382 (1992).
[23]E. Zielinski, H. Schweizer, K. Streubel, H. Eisele, and G. Weimann, J. Appl. Phys. **59**, 2196 (1986).
[24]R. Lukic-Zrnic, B. P. Gorman, R. J. Cottier, T. D. Golding, and A. G. Norman, J. Appl. Phys. **92**, 6939 (2002).
[25]W.-S. Cho, M. Luisier, D. Mohata, S. Datta, D. Pawlik, S. L. Rommel, and G. Klimeck, Appl. Phys. Lett. **100**, 063504 (2012).
[26]S. Jain and D. Roulston, Solid-State Electron. **34**, 453 (1991).